M. Onda
Mechanical Engineering Laboratory,
Agency of Industrial Science and Technology,
Ministry of International Trade and Industry,
Sakura-mura, Niihari-gun, Ibaraki-ken Japan 305

Abstract

A novel type of LTA(lighter-than-air) aircrafts has been proposed, which is designed as a control configured vehicle(CCV) and has a collision resistant and a noise abatement axisymmetric hull with a passive boundary-layer control. The hull is also made to be a control configured structure(CCS) to adapt varied load circumstances. The experimental model has a duct in the center axis of a boyant-gas holding envelope, and a small conventional thruster is installed inside the duct. Two sets of control surfaces are located to the front and rear openings of the duct, and under an appropriate control law the vehicle actively holds its stability and enhanced maneuverability performances. This paper deals with the structural design concept of the model and attitude control mechanism as well as its experimental results.

I. Introduction

Since an LTA(lighter-than-air) vehicle has a large buoyant gas bag, motion of an LTA is sluggish. LTA, however, flies in the air by the Archimedean principle, and has the least possibility of a fall due to a stall, caused by an engine shut-down or operational mistakes which can take place on other heavier-than-air aircrafts that fly by aerodynamic lift. One of major reasons why conventional LTAs have disappeared from the modern air transport market, would be unacceptable landing and take-off ground crew costs. However, nowadays sensor and robotic technologies would easily enable the construction of safe and efficient automatic take-off and landing rigs or automatic mooring masts for relatively smaller LTAs. In addition to such ground support equipment, if a personal vehicle type LTA can be developed with much improved kinetic performances, it will give useful means of transportation that may supplement automobile transport as a very safe economic vehicle.

Goldschmied[1] has proposed an efficient boundary-layer controlled(BLC) LTA hull design which yields one order of magnitude reduction of the wake drag. However, the Goldschmied body has an over-sized empennage with a long tailboom in order to get static stability, and it would not cause inconveniency since it is intended for naval airship application. And due to its rear suction BLC method, it is unable to get reverse thrust and is therefore not suitable as an inter nor intra city commuter.

In general, the more the length of an LTA becomes, the greater the increase of its moment of inertia since the moment of inertia changes according to the 5th power of the boyant-gas holding envelope length, whereas the thruster power increases according to the 2nd power of the envelope length to keep the same vehicle velocity. For this reason, smaller LTAs could have high controllability. Under this idea, a novel type of LTA was designed as a CCV and its reduction model was made and tested.

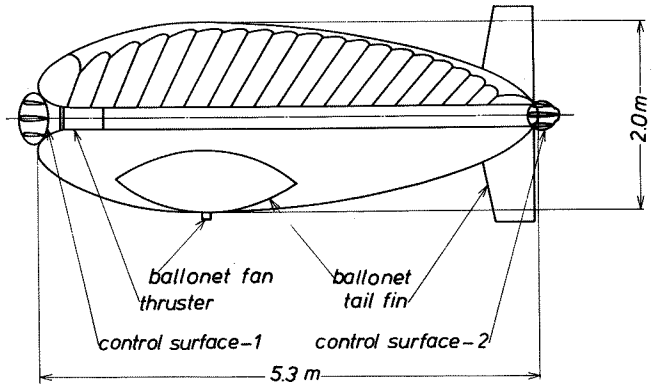

Fig.1 A novel type structured LTA aircraft

As is shown in Figure 1, the proposed reduction model has a collision resistant and a noise abatement hull with a passive boundary-layer control, and above all the hull has a control configured structure. Namely, the envelope's boyant gas pressure is controlled by an internal air bag(ballonet) in order to retain necessary hull rigidities, that is, to the extent of severities of external load conditions such as high-speed cruising or mooring under gusty weathers, boyant gas is pressurised and thereby, to prevent hazardous hull deformation and to alleviate unnecessary fatigues of the envelope skin materials as well as to decrease boyant gas leakage loss. For the realization of high performance attitude control, two sets of control surfaces are installed on the fore and aft ends of the hull and under an appropriate control law the vehicle holds its stability and enhanced maneuverability performances. This paper introduces basic design concepts, design data of the CCV model, its experimental results and the finite element method analysis of the control configured hull structure.

Design Objectives	Implemented Novel Design & Technology
1.Lower Sonic Emission	Noise Abatement Structure (Ducted Thruster in Envelope)
2.Higher Economic Speed	Boundary Layer Control (B.L.C.)
3.Collision Safe	Non-rigid Structure & Protected Thruster
4.Augmented Stability & Enhanced Maneu-verability	C.C.V. ---Centered Duct Structure ---A.C.&C.G. Locations along Thrust Line

Table 1 Design objectives and basic technologies

II. Total Design Concept

LTA's envelope has usually axisymmetric oval shape and its finess ratios 1/2.5 - 1/4 would give maximum ratios of boyancy vs. drag. The proposed boyant-gas holding hull design aims at i)augmented attitude controllability, 2)higher economic cruising speed, 3)lower power plant acoustic emission, and 4)higher anti-collision safety. As shown in Figure 2, the newly designed experimental model has a duct in the center axis of the envelope, and a thruster is installed inside the duct. Control surfaces are located to the front and rear openings of the duct. This structure enables:

1) that the aerodynamic center stays on the thruster vector line, which makes the vehicle's attitude control simpler and more effective,
2) that the thruster's intake air and downstream attack directly against control surfaces, and thereby full power is preserved for active control, and at the same time distances between the vehicle C.G. and control surfaces can be retained large, and
3) reduction of the drag coefficient by the thruster downstream application which transfers the boundary-layer separation point to the aft. This realizes higher economic vehicle speed.

The model is operated by radio-control, which enables five independent controls: two independent axis controls(pitch and yaw) each at the fore and aft ends by two sets of control surfaces plus a thruster's forward/reverse operation. The thruster consists of contra-rotating propellers driven by two DC motors. With this thruster, the vehicle attains approximately 7 meters per second as its maximum velocity.

The model's major specifications are listed in Table 2. The vehicle's inertial moments are calculated as the algebraic sum of envelope film, boyant gas, polystyrene foam made tail fins, gondola and envelope-volume-equivalent air as virtual mass.

III. Hull Structure

The hull consists of an envelope(outer gas bag), four catenary curtains with four sets of cables, a duct and a ballonet. Figure 3 presents a structure analysis model for the finite element method(FEM). In this model, the catenary curtains and some of their cables are omitted. Static analysis calculations were carried out on this model data by the NASTRAN program. The envelope and the duct are respectively divided into 480 and 360 finite elements, and the envelope elements are assumed to have panel characteristics with very small bending rigidity, since the envelope skin is membrane. The cables are considered to be rods, which only hold axial loads but no bending loads with very small torsional rigidity. The envelope sectional view is given from Equation (1) except its fore part of elliptic shape.

Fig.2 An experimental model of newly conceived LTA (The aft control surfaces are the former cruciform type.)

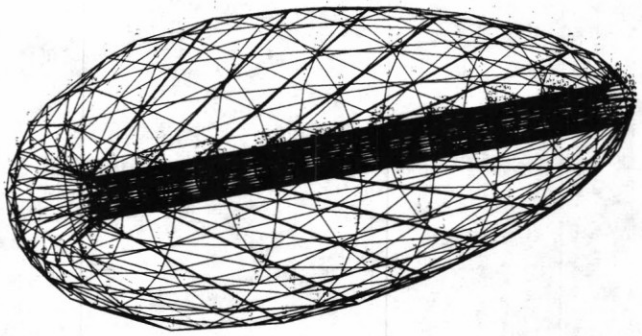

Fig.3 An FEM model for the static deformation analysis

envelope length	5.34	m
envelope diameter	2.0	m
envelope overall volume	10.9	m^3
hull surface area	26.7	m^2
total weight empty	11.5	kgf
envelope film weight	1.6	kgf
duct weight	1.8	kgf
thruster motors' rated power	each DC 12v, 10	A
maximum thrust	0.8	kgf
ballonet fan motor's rated power	DC 24v, 0.21	mA
ballonet fan maximum static pressure	9.8	mmaq.
vehicle inertial moment at its C.G. --- -- pitch, yaw, roll	46.9, 40.0, 14.2	$kgf.m.s^2$

Table 2 The experimental model's major specifications

$$r = d/2 \cdot (1+n/m)-x/l^{\,m} \cdot (1+m/n)(1-x/l)^{\,n} \qquad (1)$$

where, r= envelope radius at a distance x,
d= maximum envelope diameter,
if x/l <0.35, then m= 0.54, n= 1.00,
if x/l ≥0.35, then m= 0.30, n= 0.56,
x= horizontal distance from the nose,
l= overall length.

Figure 4 shows the model's static balance with its sectional view and one piece gore shape for manufacture. Envelope gas pressure is so controlled as to prevent possible envelope deformation in its nose part due to aerodynamic pressure, which is expressed by Equation 2. Figure 5 shows the envelope-pressure-control ballonet fan.

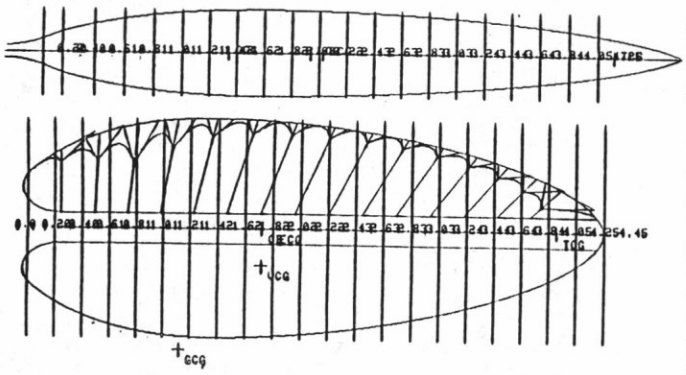

Fig.4 Static balance of the experimental model

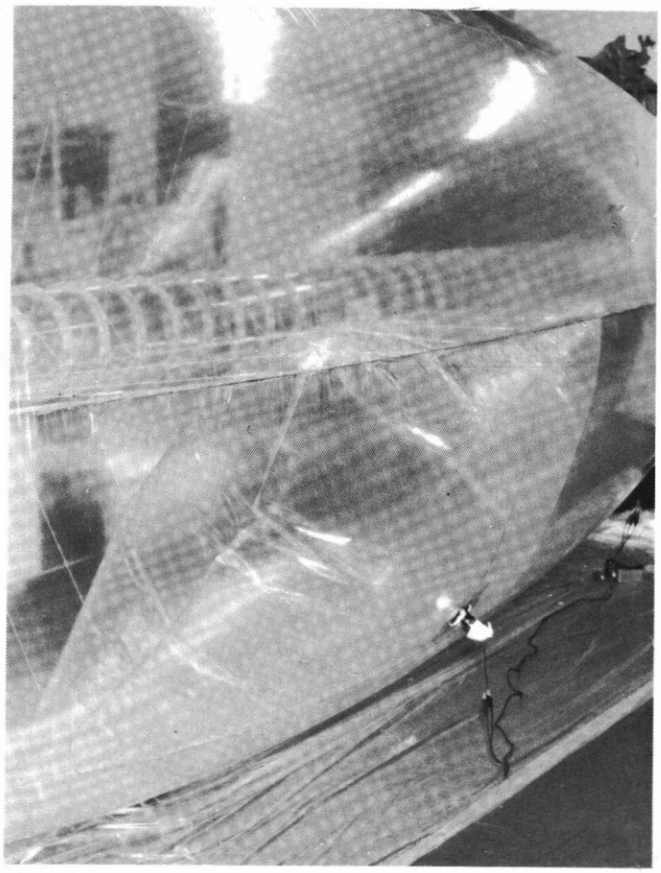

Fig.5 Pressure controlled CCS hull

$$p = 1/2 \cdot \rho \cdot v^2 \cdot C_d \cdot Q^{2/3} \qquad (2)$$

where, ρ= air density,
v= air velocity,
C_d= drag coefficient,
Q= envelope volume.

In Figure 4, triangles connected to catenary cables imply intensive cable load propagation area on the curtain. This load is incurred from the duct through the cables up to the envelope skin. The catenary cables not only support the duct in the center of the envelope but also are needed to hold the heart-shaped sectional shape of the envelope. The curtain height is determined on the supposition that the duct's static radial load should become higher from the center part to both the fore and aft ends with a parabolic distribution. A safety factor of 20 is assumed at the junction line of the curtain and the envelope. This reduction model's envelope is made of 50 μm thickness polyethylene film by welding.

The duct shown in Figure 6 is an 180 μm polyester sheet seamed cylinder reinforced with glass FRP ribs. Major difficulties of this structural style is how to design and to build a duct with high rigidity and of minimum weight. External loads to this duct will be: 1)longitudinal forces imposed by fore and aft parts of the pressurised envelope film, 2)radial and axial tensions given by the catenary cables, 3)boyant gas pressure, 4)aerodynamic pressure made by the thruster, 5)bending moments by the control surfaces and the power plant weight and its vibration, and 6)axial forces as reaction of the thruster. Among these, 4) has been found to be the most critical one, because when the thruster is swiftly switched from the maximum forward to the maximum reverse operation, it causes abrupt pressure drop inside the duct and in such a case it would squash the duct. But this tendency is totally depending on the thruster's response in case of this switching operation. The secondary prevailing load is the outer aerodynamic pressure build-up and correspondingly-controlled internal gas pressure. In Figures 7 and 8 are presented the maximum principal stresses' distribution and their stress vectors of the duct under the above load condition. From the preceding data, it is known that the approximately 20 percents from the fore duct end is exposed to the most severe stress condition, which coinsides to the physical phenomina as the above part tends to have a buckling dent at first under highly loaded condition.

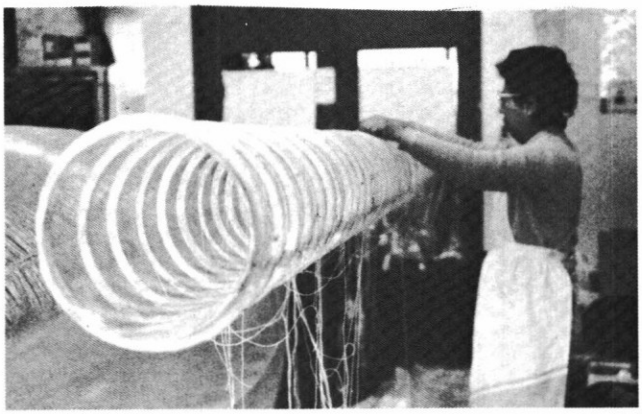

Fig.6 Polyester GFRP reinforced duct

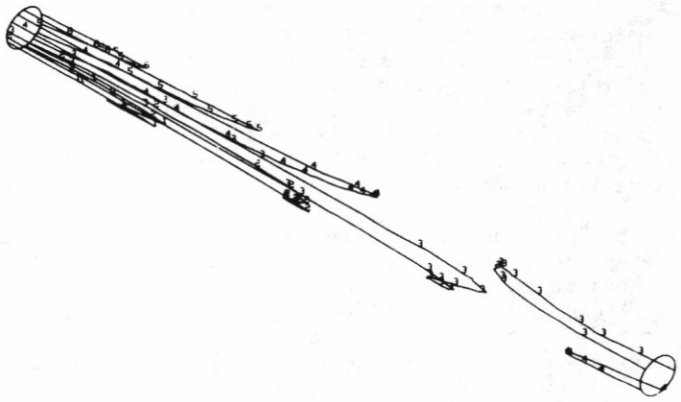

Fig.7 Maximum principal stress distributions of the duct

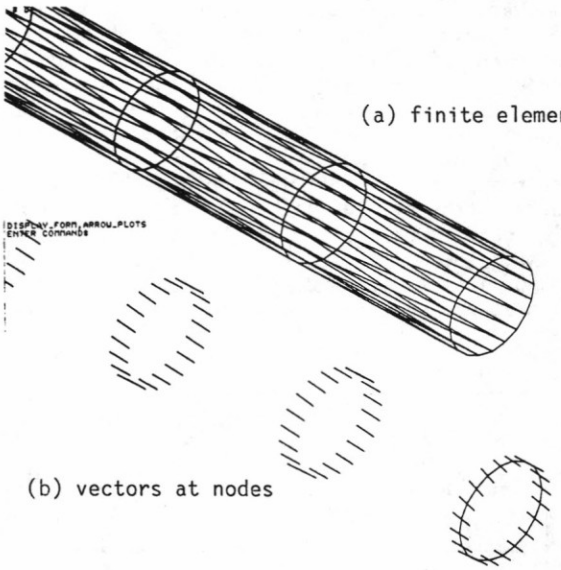

Fig.8 Maximum principal stress vectors of the duct

IV. C.C.V. Effects

Low Speed Attitude Control

For attitude control performance, as described above two sets of control surfaces are installed, which are respectively located on the fore and aft ends of the center duct. These two sets of surfaces are so designed as to produce two axial control forces for pitch and yaw attitude controls, by receiving thruster intake and ejecting air flow. As is shown in Figure 9, each of the control surfaces is supported by a gimbal frame and this makes two axial rotation of the control surfaces. A set of control surfaces is again made by two groups of three parallel aerofoils and each group's aerofoils cross to the other group's aerofoils perpendicularly. These sets of control surfaces are respectively supported at their aerodynamic centers by the gimbal frames and further by stays from the center duct, which is shown in Figure 10, and a set of control surfaces is independently driven by two servomotors regarding its horizontal and perpendicular axes. In Figure 11, these novel control surfaces' performance data are shown, in which lateral control forces produced by two sets surfaces are calculated as a combined value which

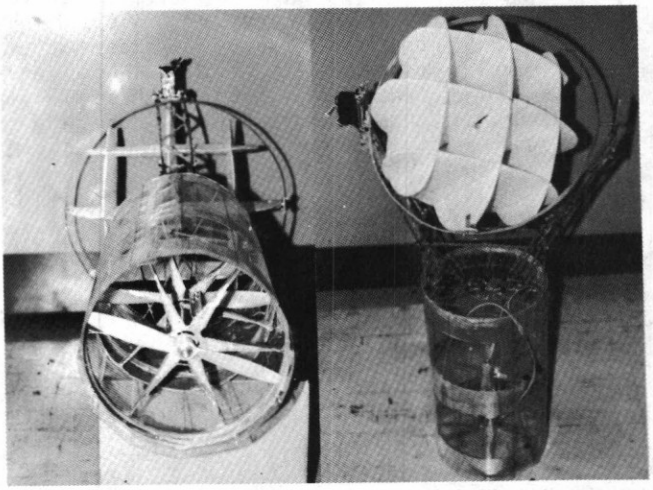

Fig.9 Gimbal typed two-axial control surfaces with contra-rotating propeller

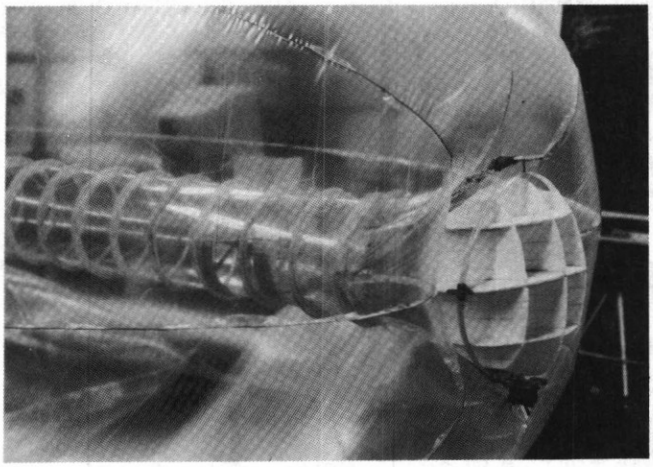

Fig. 10 Fore control surfaces installed at the fore duct end

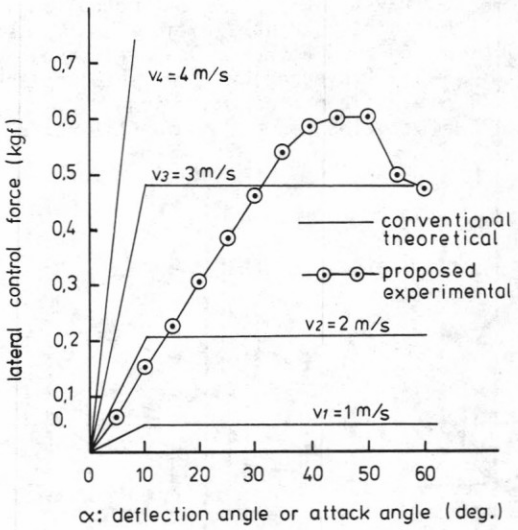

Fig. 11 Control surface deflection angle vs. lateral control force

is equivalent at the aft end. The theoretical data show lateral forces which would be yielded by conventionally designed control surfaces whose surface area is determined by envelope length and volume.[2] These data imply that with these novel control surfaces this experimental model can have a fairly good attitude control ability in the zero vicinity of the air speed.

Active Stability Control

A control-configured vehicle is designed unstable to reserve higher kinetic performances, and in order to attain stability at a higher vehicle speed active control is introduced. In this model, active control is realized by utilizing rate gyros and two kinds of control surfaces: ones fixed on stabilizers and the other gimbaled ones. Appropriate feedback control gains are searched through simulation study.

Computer simulations are carried out regarding the vehicle's longitudinal dynamics by the Runge-Kutta method. Three dimensional dynamic analysis would have to be analyzed. But this makes mathematical formulation complicated and, in this model the most difficult control dimension is longitudinal as far as the vehicle's stability is concerned. Therefore the only longitudinal dynamics are dealt with here.

The following formulae are the basic descriptions of the model's longitudinal motion. A simplified model of the vehicle and state variables and parameter values are indicated in Figure 12. In this way, any design features of the experimental model can be expressed by choosing parameter values of the described mathematical model.

$$\frac{W}{g}\cdot\dot{V} = (B-W)\cdot\sin\gamma + F\cdot\cos(\alpha+\delta) - D_e \qquad (3)$$

$$\frac{W}{g}\cdot V\cdot\dot{\gamma} = (B-W)\cdot\cos\gamma + F\cdot\sin(\alpha+\delta) + L_e \qquad (4)$$

$$I\cdot\ddot{\theta} = M_{CG} \qquad (5)$$

where, W= weight, B= boyancy,
V= velocity, F= control force,
g= gravity, δ= control angle,
γ= flight path inclination,
α= angle of attack, D_e= drag(envelope),
L_e= lift(envelope), θ= vehicle pitch,
M_{CG}= vehicle moment regarding C.G.,
I= vehicle's moment of inertia re:C.G.

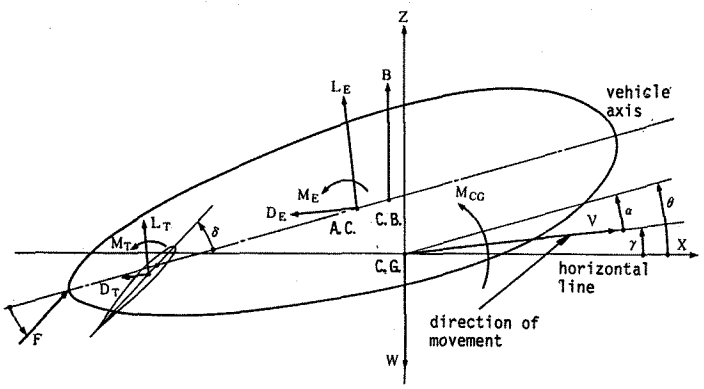

Fig. 12 Simplified model and physical value notation

M_{CG} in Equation (5), a moment regarding the vehicle C.G. can be largely classified into moments by envelope's aerodynamic effects, by tailfins, and by thrust of the power plant. Moments created by the two kinds of control surfaces are respectively moments effected only by the vehicle's external air flow and moments by these surfaces exposed to the thruster's down wash.

Number of simulation runs are carried out on various different parameter values and their combinations. Among these, Two phase plain diagrams in Figure 13 show two different transient responses regarding the vehicle's pitching motion; one for unstable and the other stable one after searching a stable combination of parameters. In these phase plain diagrams, the abscissae are pitch angle and the other coordinates indicate angular pitching velocity. In these simulation runs, the thruster power is set to be almost maximum and minimum stabilizer surface area is introduced in order to attain stability boundary to a level that search would be able to find the optimum feedback gain of the rate gyro.

Figure 14 shows the vehicle's velocity changes in the above cases; the upper graph shows unstable before the parameter optimization and the lower one is after attained stability. As it is seen, the stable case does not lose kinetic power and maintains the same velocity during the correction period of initial attitude errors. To the contrary the unstable case keeps losing its cruising speed.

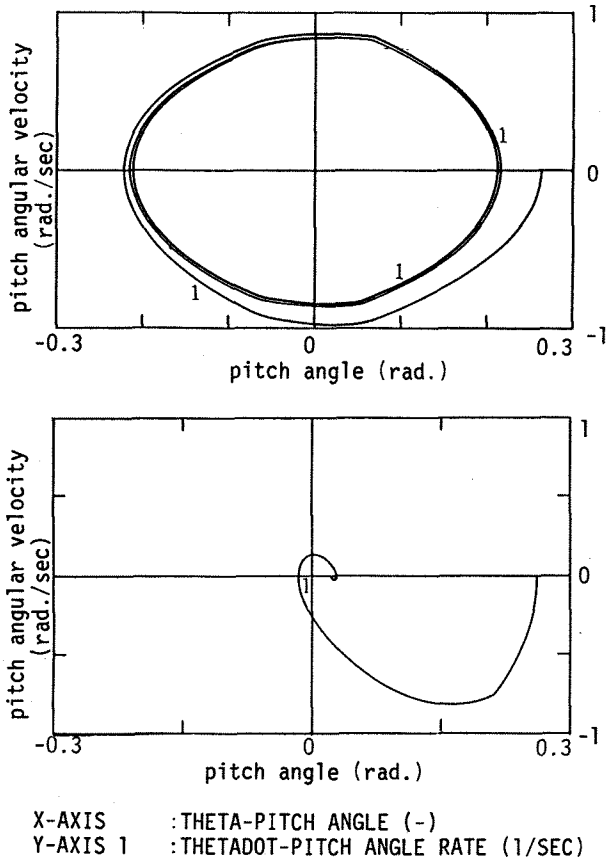

Fig. 13 Phase plain diagrams of pitching motion

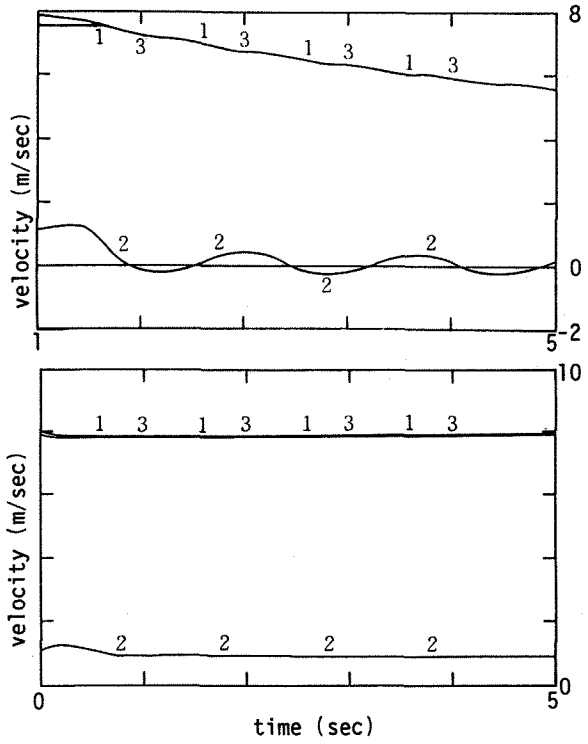

X-AXIS :TIME (SEC)
Y-AXIS 1 :HORIZONTAL VELOCITY COMPONENT (M/SEC)
Y-AXIS 2 :VERTICAL VELOCITY COMPONENT (M/SEC)
Y-AXIS 3 :VELOCITY ALONG MOTION DIRECTION (M/SEC)

Fig.14 Vehicle velocity in time domain

VI. Boundary-Layer Control Effects

The boundary-layer control effect was measured up to an 80 km/hr airspeed by towing the model with an automobile. Therefore the fabricated model has a Reynolds number of 7.4×10^6. Figure 10 shows the BLC effect. These data shows that the BLC effects are not large as to the degree of the Goldschmied body. In order to reduce the induced drag by tailfins, the minimum stabilizer area was determined after installing the active control.

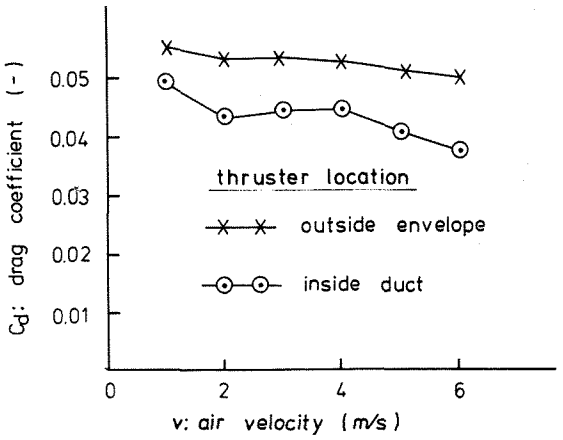

Fig.15 Drag coefficient vs. air velocity (attack angle=0)

VII. Conclusion

A novel type of LTA hull with a new attitude control system was designed and its reduction model was fabricated and tested. The hull as CCS is good to make the structure materials duarable and is effective to the objectives of the proposed design concept. The combination of two control surfaces augments the vehicle's maneuverability at take-off and landing speeds and the stability at higher cruising speed as well. Thereby C.C.V. concept has been realized. The BLC effect was experimentally proven not remarkable.

References

(1) F. R. Goldschmied, Wind tunnel demonstration of an optimized LTA system with 65% power reduction and neutral static stability. AIAA Lighter-than-air Systems Conference Collection Papers. (July 25-27, 1983) pp.77-88

(2) H. Sekine, Airship Technology, Togaku-sha press, (may 1935) pp.162-163